THE EFFECT OF SIZE OF NON-METALLIC INCLUSION ON THE DUCTILE FRACTURE BEHAVIOUR OF PURE IRON

T. Kunio, M. Shimizu and Y. Kobayashi*

INTRODUCTION

In many experimental [1] and theoretical [2] works on ductile fracture of metals, much attention has been paid to the influence of volume fraction of hard second phase particles upon ductility. However, some evidence that the size [3] and shape [4] of the particle involved may affect ductility and failure mechanisms has been reported recently. Some other variables, such as the composition and distribution of the particles, will be important also. Consequently, consideration of the effect of particles must be independent of the other variables which may influence ductile fracture behaviour.

Thus, the present work was undertaken to establish the effect of size of non-metallic inclusion upon void and dimple formation in pure iron deformed plastically at room temperature, with emphasis on the critical size of inclusion leading to void and dimple nucleation.

EXPERIMENTAL PROCEDURE

Material and Testing

Cylindrical specimens of 20 mm length and 5 mm diameter were prepared from an electrolytic iron (Table 1) containing only FeO type inclusions with spherical shape. Before and after machining the specimens were annealing in vacuo in two ways, at 1073K for 2 hours and at 1173K for 3 hours. Tensile tests were carried out using a testing machine of Olzen type at a nominal strain rate of 1×10^{-3} sec^{-1}, which was reduced to a very low value of 2×10^{-5} sec^{-1} just before the final fracture, for the purpose of minimizing the number of inclusions dropped out of the fracture surface. Average grain size was 200 μm. Ultimate tensile stress and yield stress were 258 MPa and 98.1 MPa, respectively. Fracture ductility is 1.65.

Techniques of Metallography and Fractography

The size distribution of inclusions was obtained, using three types of quantitative microscopy method, on three different test planes [5]; (i) mechanically polished section, (ii) artificially introduced cleavage facet and (iii) surface replicated for extraction of inclusions. Examples of inclusions appearing on each test plane are shown in Figure 1. It should be noted that inclusions in Figures 1(a) and (b) will not show their true diameters but merely give the diameters of circles of their intersections with the test plane. The size distribution of these circles was converted to the true size distribution of inclusions using both Saltikov's method [6] and Fullman's equation [7]. On the other hand, Figure 1(c) gives the

*Keio University, Yokohama, Japan.

true diameters of particles, because the first treatment of etching for the preparation of extraction replica was conducted very carefully so that the depth of removed layer might exceed the maximum inclusion radius. For the purpose of oberving microvoids which had been generated near the fracture surface, the broken specimens were immersed in liquid nitrogen and then fractured in a brittle manner along a slit introduced artificially, the plane of which was parallel to the tensile axis. The voids appearing on the cleavage facets were examined by a scanning electron microscope. The significant advantages of the above may be described as follows; the [110] direction in each grain near the necked part of the specimen tends to be altered toward the tensile axis [8] as tensile deformation proceeds, thus a texture with preferred orientation is formed. Consequently, the procedure enabled us to examine the behaviour of voids on the cleavage facets parallel to the tensile axis in a microscopic sense.

The centre part of the fracture surface was examined with a scanning electron microscope from the direction parallel to the tensile axis at magnifications of x4000 and x8000, to see how the size of dimple is related to that of the inclusion.

Dimples on the fracture surface may be divided into the following three types; normal type, elongated type and mixed type. The size of the normal dimple was evaluated by the diameter D_D of the circle having an area A_D equal to that of the zone enclosed by the chisel edge of dimple appearing on the microphotograph. $N_{AID}(D_I)$, the number of inclusions having true diameter D_I on the unit area of dimple containing inclusion, was obtained immediately from the data measured on the microphotograph.

In this study, microphotographs were taken with three different types of microscope; optical, scanning electron and transmission electron. The accuracies of their magnification were within ±3%.

RESULTS AND DISCUSSIONS

Size Distribution of Inclusions

The size distribution of inclusions in the iron studied is shown in Figure 2. $N_{AI}(D_I)$ represents the number* of inclusions having a diameter of D_I on the unit area of test plane, where D_I stands for the representative value of all inclusion diameters ranging from $D_I-\Delta D_I$ to D_I, because the actual diameters of inclusions were distributed continuously in the range of 0.05 to 4 μm in which ΔD_I is the size class interval of inclusion.

The values of $N_{AI}(D_I)$ deduced from the different measuring procedures mentioned above do not necessarily agree quantitatively. A log-normal approximation curve is given in Figure 2 as the representative curve of $N_{AI}(D_I)$, since the data obtained by use of extraction replicas are considered to be the most reliable of the three [9]. The total volume fraction of inclusion, V_{VI}, was estimated to be 0.60% from $N_{AI}(D_I)$ through Fullman's equation [7].

*It is obvious that $N_{AI}(D_I)$ is dependent upon the adopted value of ΔD_I. So that, in Figure 2 the measured values of $N_{AI}(D_I)$ by 1st procedure (ΔD_I = 0.5 μm) have been converted into those corresponding to ΔD_I = 0.125 μm in 2nd and 3rd procedures.

Behaviour of Void Growth

Figure 3(a), (b), (c) are scanning electron micrographs showing the voids observed on the cleavage facets. From these figures, it is obvious that most voids are formed through debonding of the interface between the inclusion and the matrix, and that the void growth occurs preferentially in the direction of the tensile axis. These observations of void growth in iron are closely analogous to those of Palmer et al. [3] for copper.

The successive coalescence of voids may lead to the initiation and propagation of a macroscopic crack, resulting in the creation of dimples on the final fracture surface.

Dimples and Inclusions

The fracture surface produced by tensile testing was fully covered with dimples, the majority of which contain inclusions, as seen in Figure 4. Figure 5 shows the relationship between the sizes of dimples and inclusions for the case of normal dimples. It turns out from the figure that the large inclusion causes the dimple to be larger, and the following relationship holds,

$$D_D(D_I) \propto D_I \qquad (1)$$

The experimental results concerning the size distribution of inclusions $N_{AID}(D_I)$ on the fracture surface are shown in Figure 6. Inclusions having a diameter D_I of about 0.5 μm are most frequently observed on the fracture surface. The present material, however, contains a tremendous number of inclusions having diameters less than 0.5 μm, as shown in Figure 2. Therefore, comparison of Figure 6 with Figure 2 will reveal that inclusions having diameters smaller than about 0.1 μm will not actually take part in dimple formation. It should be noted that the results in Figure 6, which were constructed from measurement only of the dimples containing inclusions, will not necessarily indicate the actual size effect of inclusions in dimple formation, because some inclusions must have been lost from the dimples. Discussions on this point follows.

It was confirmed previously that most dimples are initiated from inclusions in this material [9], and that the size of dimple is proportional to that of the inclusion, as seen in Figure 5. In other words, there exists one-to-one correspondence between sizes of inclusion and dimple. Consequently, the size effect of inclusions on dimple formation will be successfully examined by measuring the sizes of dimples without direct measurement of inclusions. The following procedure suffices to verify whether or not the loss of inclusions from dimples effects $N_{AID}(D_I)$. Two kinds of dimple size distributions were measured independently; one was $N_{ADI}(D_D)$ representing the size distribution of dimples in which inclusions are observed, the other is $N_{AD}(D_D)$ representing that measured irrespective of the presence of inclusions. The values of $N_{ADI}(D_D)$ and $N_{AD}(D_D)$ may agree with each other only if no inclusions have been lost from dimples or inclusions of all sizes have been lost at the same rate. Since the former is not conceivable, the latter is considered to be the case. Figure 7 shows that the observed values of $N_{ADI}(D_D)$ and $N_{AD}(D_D)$ are in good agreement.

It is confirmed from the above that, without any additional processing, the result shown in Figure 6 indicates immediately the actual size effect of inclusions which have taken part in dimple formation. Consequently,

it is concluded that any small inclusion of size below about 0.1 μm will not take part in dimple formation.

For the purpose of making a more quantitative interpretation of the size effect of inclusions on dimple formation, a parameter $R(D_I)$ is introduced, defined by:

$$R(D_I) = \frac{N_{AID}(D_I)}{N_{AI}(D_I)} \qquad (2)$$

The parameter $R(D_I)$ may be interpreted as follows.

The case $R(D_I) = 0$ indicates that a dimple will not be formed at the site of the inclusion having diameter D_I, because $N_{AID}(D_I) = 0$ in equation (2). In other words, fracture will not be associated with an inclusion of this size. When $R(D_I) = 1$, $N_{AID}(D_I)$ is equal to $N_{AI}(D_I)$. This means that the distribution of inclusion size in the virgin material is identical with that measured on the fracture surface; in other words, inclusions with size D_I appear on the fracture surface at the same frequency as that expected on an arbitrary test plane. Therefore, $R(D_I) = 1$ indicates that the location of the fracture surface is not affected by inclusions of size D_I. The case $R(D_I) > 1$ means that inclusions of size D_I appear on the fracture surface at a higher frequency than that expected on the test plane.

Now the value of $R(D_I)$ can be calculated from equation (2). To obtain a value for $N_{AI}(D_I)$, the experimental result given in Figure 2 is available. An approximate value of $N_{AID}(D_I)$ may be obtained from the experimental results given in Figure 6. This is an approximation because the values of $N_{AID}(D_I)$ in Figure 6 are not strictly correct, being determined from measurements not along the jagged fracture surface, but on the flat micrograph.

The calculated value of $R(D_I)$ from the observed values is shown in Figure 8. $R(D_I)$ increases sharply with increase of D_I in the range 0 - 0.5 μm, and it tends to a constant value larger than unity when D_I is larger than 1 μm. This means that inclusions larger than 1 μm, whose number on the fracture surface is much more than that expected on an arbitrary test plane, actually take part in the creation of the fracture surface. It also indicates that the ductile crack will propagate preferentially through the sites of the comparatively larger inclusions. On the other hand, inclusions smaller than 0.1 μm, although they exist in the material, will not appear on the fracture surface. Thus it can be concluded that the minimum size, i.e. the critical size of an inclusion leading to dimple formation is about 0.1 μm.

CONCLUSIONS

The role of second phase particles in ductile fracture behaviour, in terms of the effect of size of inclusions on void and dimple formation was studied by quantitative metallography in a pure iron containing spherical FeO type inclusions.

The conclusion obtained can be summarized as follows:

1. The size distribution of FeO type inclusions in the pure iron could be described approximately by a logarithm normal curve in the range of 0.05 to 4 μm in size. In the ductile fracture process, it was observed that voids were initiated through the separation of the boundary between the inclusion and matrix. Voids grow preferentially in the direction of the tensile axis with increase of bulk deformation of the specimen.
2. It was found that the minimum size of inclusions which can take part in dimple formation is about 0.1 μm. The size of a dimple containing an inclusion is proportional to the size of the inclusion involved.
3. The application of quantitative fractography by using the newly introduced parameter $R(D_I)$ shows that the ductile fracture surface is produced as a consequence of the preferential propagation of a ductile crack passing through the sites of the larger inclusions.

ACKNOWLEDGEMENTS

The authors wish to thank Mr. M. Tsujimoto, Kawasaki Heavy Industries Ltd., Mr. A. Misawa, Japanese National Railways and Mr. Sakamoto, Kansai Paint Co. Ltd., for their diligent technical care in carrying out the experiments.

REFERENCES

1. EDELSON, B. I. and BALDWIN, M., Jr., Trans. ASM, 55, 1962, 230.
2. THOMASON, P. F., J. Inst. Metals, 96, 1968, 360.
3. PALMER, I. G. and SMITH, G. C., 2nd Bolton Landing Conf. on Oxide Dispersion Strengthening, Lake George, 1966, 253.
4. PICKERING, F. B., Proc. Int. Conf. Toward Improved Ductility and Toughness, Kyoto, 1971, 9.
5. DEHOFF, R. T. and RHINES, F. N., "Quantitative Microscopy", McGraw-Hill, 1968, 37.
6. SALTYKOV, S. A., "Stereometric Metallography", (2nd ed.), Metallurgizdat, 1958, 446.
7. FULLMAN, R. L., Trans. Metallurg. Soc. AIME, 197, 1953, 447.
8. KUNIO, T. and KOBAYASHI, Y., Preprint of Japan Soc. Mech. Engrs. (in Japanese), No. 734-3, 1973-3, 7.
9. KOBAYASHI, Y., Doctoral Thesis, Keio University, 1974.

Table 1 Chemical Composition

C	Si	Mn	P	S	Al	N	O
0.008	0.034	0.0025	0.0014	0.007	0.002	0.0029	0.062

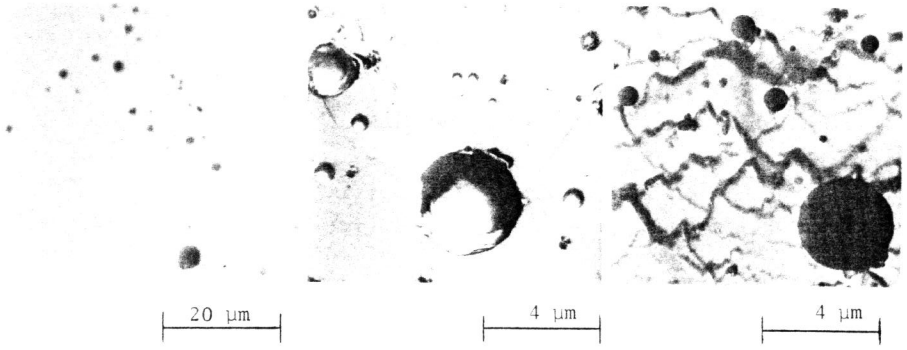

Figure 1 Three Kinds of Observations of Inclusions

(a) On the Polished Section (First Method)
(b) On the Cleavage Facet (Second Method), and
(c) On the Extraction Replica (Third Method)

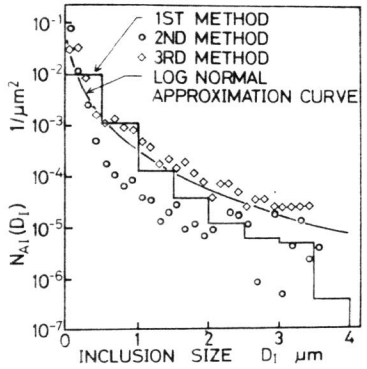

Figure 2 Size Distribution of Inclusions

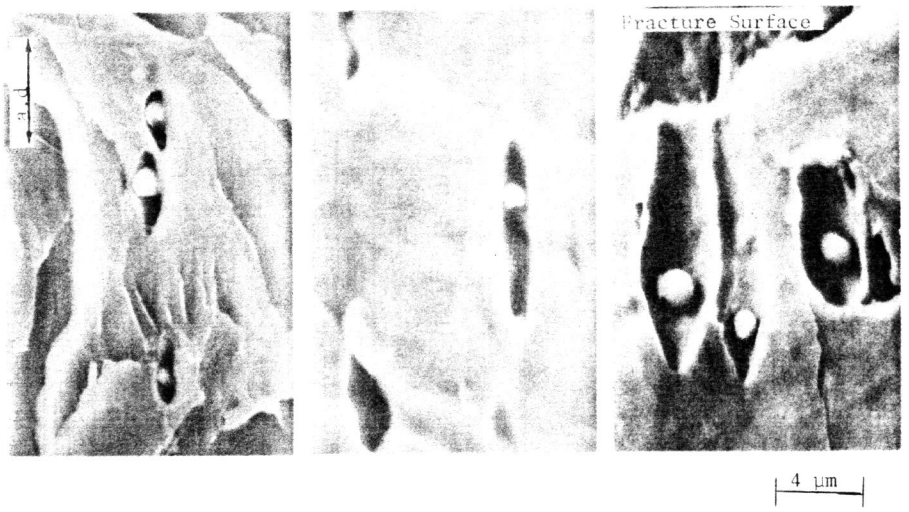

Figure 3 Feature of Void Growth on the Cleavage Facet Introduced Artificially

(a) At the Distance of about 1 mm Beneath the Fracture Surface,
(b) At the Distance of about 0.5 mm Beneath the Fracture Surface,
(c) In the Vicinity of Fracture Edge

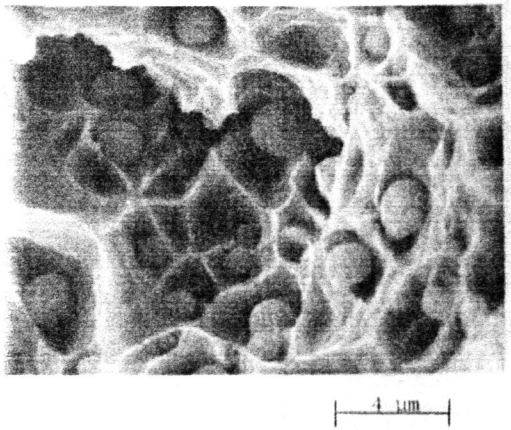

Figure 4 Appearance of Inclusions in Dimples

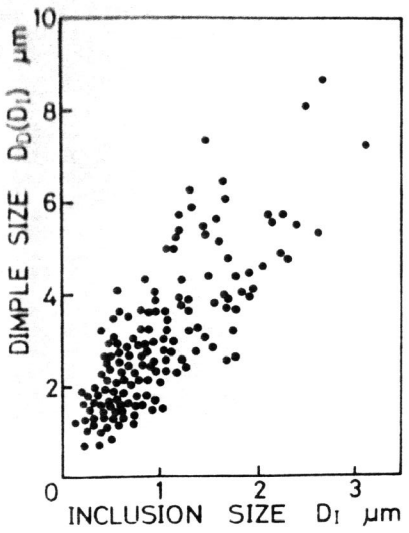

Figure 5 Relationship Between Sizes of Dimple and Inclusion

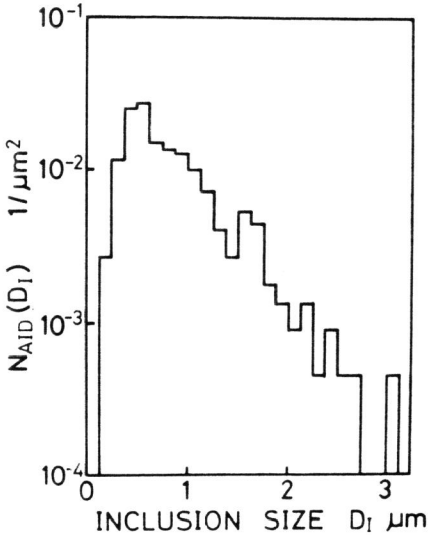

Figure 6 Size Distribution of Inclusions on Fracture Surface

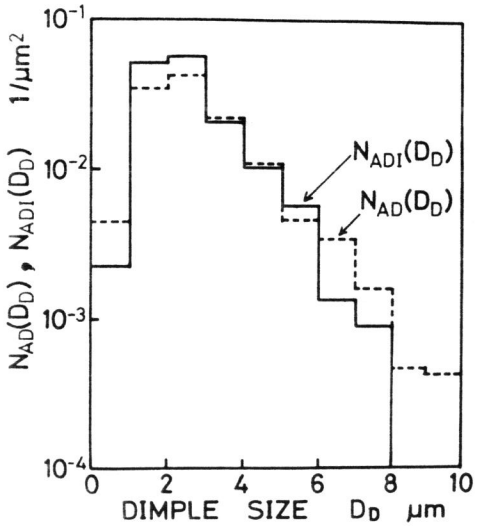

Figure 7 Comparison of $N_{AD}(D_D)$ with $N_{ADI}(D_D)$

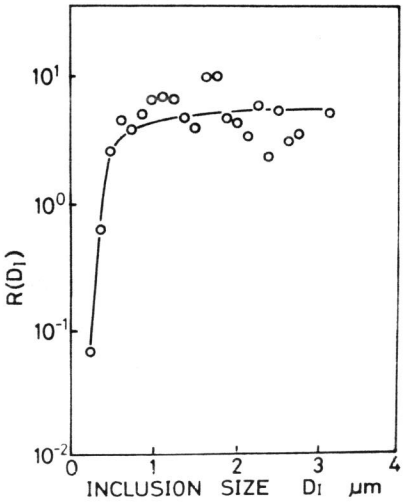

Figure 8 Relationship Between $R(D_I)$ and D_I